Acta Pharmaceutica Sinica B 2023;13(8):3352−3364

Chinese Pharmaceutical Association
Institute of Materia Medica, Chinese Academy of Medical Sciences

Acta Pharmaceutica Sinica B

www.elsevier.com/locate/apsb
www.sciencedirect.com

ORIGINAL ARTICLE

Hepatic DDAH1 mitigates hepatic steatosis and insulin resistance in obese mice: Involvement of reduced S100A11 expression

Xiyue Shen[a,b,†], Kai Luo[a,†], Juntao Yuan[a,†], Junling Gao[a], Bingqing Cui[a], Zhuoran Yu[a], Zhongbing Lu[a,*]

[a]*College of Life Science, University of Chinese Academy of Sciences, Beijing 100049, China*
[b]*Institute of Respiratory Medicine, Tongji University School of Medicine, Shanghai 200433, China*

Received 15 January 2023; received in revised form 16 March 2023; accepted 3 April 2023

KEY WORDS

ADMA;
DDAH1;
Hepatic steatosis;
Insulin resistance;
S100A11;
Oxidative stress;
Inflammation;
High fat diet

Abstract Dimethylarginine dimethylaminohydrolase 1 (DDAH1) is an important regulator of plasma asymmetric dimethylarginine (ADMA) levels, which are associated with insulin resistance in patients with nonalcoholic fatty liver disease (NAFLD). To elucidate the role of hepatic DDAH1 in the pathogenesis of NAFLD, we used hepatocyte-specific *Ddah1*-knockout mice (*Ddah1*^{HKO}) to examine the progress of high-fat diet (HFD)-induced NAFLD. Compared to diet-matched flox/flox littermates (*Ddah1*$^{f/f}$), *Ddah1*^{HKO} mice exhibited higher serum ADMA levels. After HFD feeding for 16 weeks, *Ddah1*^{HKO} mice developed more severe liver steatosis and worse insulin resistance than *Ddah1*$^{f/f}$ mice. On the contrary, overexpression of DDAH1 attenuated the NAFLD-like phenotype in HFD-fed mice and *ob*/*ob* mice. RNA-seq analysis showed that DDAH1 affects NF-κB signaling, lipid metabolic processes, and immune system processes in fatty livers. Furthermore, DDAH1 reduces S100 calcium-binding protein A11 (S100A11) possibly *via* NF-κB, JNK and oxidative stress-dependent manner in fatty livers. Knockdown of hepatic S100a11 by an AAV8-sh*S100a11* vector alleviated hepatic steatosis and insulin resistance in HFD-fed *Ddah1*^{HKO} mice. In summary, our results suggested that the liver DDAH1/S100A11 axis has a marked effect on liver lipid metabolism in obese mice. Strategies to increase liver DDAH1 activity or decrease S100A11 expression could be a valuable approach for NAFLD therapy.

*Corresponding author. Tel./fax: +86 10 69672630.
E-mail address: luzhongbing@ucas.ac.cn (Zhongbing Lu).
†These authors made equal contributions to this work.

Peer review under the responsibility of Chinese Pharmaceutical Association and Institute of Materia Medica, Chinese Academy of Medical Sciences.

https://doi.org/10.1016/j.apsb.2023.05.020

1. Introduction

Nonalcoholic fatty liver disease (NAFLD), the most common liver disease, is defined as a metabolic disease with a diagnostic hallmark of accumulation of liver triglycerides (TG) above 5% without heavy alcohol consumption[1]. NAFLD is associated with a series of metabolic syndromes, including insulin resistance, obesity, diabetes, and dyslipidemia[2]. The pathogenesis of NAFLD is very complex, and the most widely accepted mechanism is the "multiple hit" hypothesis. In this hypothesis, steatosis occurs first, followed by multiple insults, including oxidative stress, inflammation, intestinal microflora, nutritional factors, and genetic and epigenetic factors that promote the progression of steatosis to steatohepatitis[3]. During the past twenty years, the increasing worldwide prevalence of NAFLD has become a global health problem[4,5]. Unfortunately, there are still no effective therapeutic options for NAFLD.

Asymmetric dimethylarginine (ADMA) and its metabolizing enzyme, dimethylarginine dimethylaminohydrolase 1 (DDAH1), have been proposed to be involved in the pathogenesis of NAFLD by regulating nitric oxide synthase activity. In patients with NAFLD, plasma ADMA levels are elevated, which could cause systemic endothelial dysfunction and insulin resistance (IR)[6–8]. DDAH1 is highly expressed in the liver, and liver DDAH1 exerts a profound effect on circulating ADMA levels[9,10]. As a target gene for the farnesoid X receptor, hepatic DDAH1 can be upregulated by farnesoid X receptor agonists[10,11], which could be promising agents for treating NAFLD[12]. Recently, we demonstrated that global *Ddah1* deficiency exacerbates high-fat diet (HFD)-induced hepatic steatosis and IR[13]. However, the detailed mechanisms of the functions of DDAH1 in hepatocytes are still largely unknown.

In this study, we investigated the tissue-specific role of DDAH1 in the pathogenesis of NAFLD using hepatocyte-specific *Ddah1 knockout* mice ($Ddah1^{HKO}$). We also used DDAH1 transgenic mice (DDAH1-TG) and recombinant adeno-associated virus serotype 8 (AAV8) to overexpress DDAH1 in the livers of leptin-deficient (*ob*/*ob*) mice to confirm the protective effect of DDAH1 on NAFLD.

2. Materials and methods

2.1. Mice

The $Ddah1^{f/f}$ mice[14] were kindly provided by Dr. Yingjie Chen from the University of Minnesota (St. Paul, MN, USA). Alb-ERT2-Cre and *ob*/*ob* mice were purchased from Beijing Vitalstar Biotechnology Co., Ltd. (Beijing, China) and HFK Bioscience Co. (Beijing, China), respectively. DDAH1-TG mice[15] (C57BL/6J background) were generated by Cyagen Biosciences Inc. (Jiangsu, China). $Ddah1^{f/f}$ mice were crossed with Alb-ERT2-Cre mice for at least four generations. To obtain $Ddah1^{HKO}$ mice, the $Ddah1^{f/f;alb\text{-}ERT2\text{-}cre/+}$ and $Ddah1^{f/f;+/+}$ littermates (used as control, hereafter referred to as $Ddah1^{f/f}$) at the age of 6−8 weeks were administered tamoxifen (50 mg/kg) by intraperitoneal injection once every 24 h for a total of 5 consecutive days.

To induce hepatic steatosis, 8-week-old male mice were randomly divided into 2 groups (10 mice/group) and fed with either regular chow (RC) (HFK Bioscience; 7.5% kcal fat) or HFD (Research Diet, #D12492; 60% kcal fat) *ad libitum* for 16 weeks.

The pAAV-U6-GFP vector with a shRNA sequence targeting *S100a11* (GCGGGAAGGATGGAAACAACAT) was used for viral packaging. AAV8-sh*S100a11* and AAV8 vectors with a liver-specific promoter (thyroxine-binding globulin)-driven expression of a histidine tag (HIS) or human DDAH1 cDNA were produced by Vigene Biosciences Inc. (Shandong, China). Hepatic DDAH1 overexpression in *ob*/*ob* mice and hepatic *S100a11* knockdown in HFD-fed mice were achieved by tail vein injection of AAV8-h*DDAH1* and AAV8-sh*S100a11* (1.1×10^{12} vg/mouse), respectively. Four weeks after injection, the mice were sacrificed, and their tissues were harvested.

Animal studies were carried out according to the *Guide for the Care and Use of Laboratory Animals (Eighth edition, 2011)* and the approval of the Animal Care and Use Committee of University of Chinese Academy of Sciences.

2.2. Measurements of serum and liver biochemical markers

Serum alanine aminotransferase (ALT), aspartate aminotransferase (AST), triglyceride (TG) and cholesterol were measured with kits from Nanjing Jiancheng Bioengineering Institute (#C009-2, #C010-2, #A110-2-1, and #A111-1, Jiangsu, China). Serum levels of ADMA and leptin were measured with ELISA kits from Bio-Techne Co., Ltd. (#NBP2-66728 and #MOB00, Minneapolis, MN, USA). Liver TG and cholesterol were measured with kits from Applygen Technologies Inc. (#E1013 and #E1015, Beijing, China). Serum insulin levels were measured using an ALPCO ultrasensitive insulin ELISA kit (#80-INSMSU-E01, ALPCO Diagnostics, Salem, NH, USA). A Roche Accu-Chek® glucometer (Roche Diagnostics, Indianapolis, IN, USA) was used for blood glucose measurement. Oral glucose tolerance tests (OGTT) were performed using an oral gavage of 1 g/kg glucose after overnight fasting. Insulin tolerance tests (ITT) were performed *via* intraperitoneal injection of 0.5 U/kg insulin after fasting for 4 h. For the *ob*/*ob* group, the insulin concentration was raised to 2 U/kg.

2.3. Histological analyses

Mouse liver paraffin sections (5 μm) were stained with hematoxylin and eosin (H&E) to assess liver steatosis. Frozen liver sections (4 μm) were stained with oil red O or DHE for 30 min to assess lipid accumulation and superoxide generation, respectively.

2.4. Analysis of gene expression profile

Total RNA was extracted from the livers of HFD-fed mice using TRIzol reagent, and RNA integrity was checked using an Agilent 2100 bioanalyzer (Thermo Fisher Scientific, MA, USA). After further purification, the RNA samples were used for library construction. RNA sequencing was performed on a BGISEQ500 platform (BGI-Shenzhen, China). The differentially expressed genes (DEG) between the two groups were determined as previously described[16].

RNA extracted from the livers of HFD-fed WT and $Ddah1^{-/-}$ mice was also analyzed with an Agilent whole mouse genome oligo microarray (4×44 K) (Agilent Technologies, Santa Clara, CA, USA).

The Kyoto Encyclopaedia of Genes and Genomes (KEGG) enrichment analysis was performed using the phyper function of the R software. The P value was adjusted for the false discovery rate to obtain the q-value, and a q-value ≤ 0.05 was considered significant enrichment.

2.5. Cell culture

The detailed protocol for the isolation and culture of primary hepatocyte were described in a previous report[17]. The protocol for HepG2 and HEK293 cell culture and palmitic acid (PA) treatment (0.25 mmol/L, 24 h) was described in our previous studies[13,18]. The steatosis and intracellular ROS levels were determined by fluorescence microscopy using Nile Red and CellROX™ Deep Red, respectively. After the treatment, cells were washed with PBS and incubated with 1 μmol/L fluorescence dyes (final concentration) at 37 °C for 15 min. The cells were washed three times with ice-cold PBS and then imaged using Zeiss fluorescence microscopy (Zeiss, Oberkochen, Germany). The concentrations of inhibitors or chemicals used were QNZ (50 nmol/L, Selleck Chemical, Houston, TX, USA, #S4902), SP600125 (50 nmol/L, Selleck Chemical, #S1460), *N*-acetylcysteine (NAC, 5 mmol/L, Selleck Chemical, #S1623) and ADMA (10 μmol/L, Sigma Chemical Co., #D4268). The luciferase activity of the S100A11 promoter was measured using the Beyotime dual luciferase assay kit (Beyotime Institute of Biotechnology, Shanghai, China, #RG027).

2.6. Western blot and quantitative real-time PCR analysis

Protein extraction and Western blot were performed as previously described[19]. Detailed information on primary antibodies used in this study is listed in Supporting Information Table S1.

An SYBR® Premix Ex Taq™ II kit (#RR820A, TaKaRa, Otsu, Japan) was used for the quantitative real-time polymerase chain reaction (qPCR) assay and the results were normalized to 18S rRNA. The gene-specific primers used in this study are listed in Supporting Information Table S2.

2.7. Statistical analysis

All data are expressed as mean ± standard error of mean (SEM) and were analyzed with GraphPad Prism 8 (GraphPad Software Inc., CA, USA). An unpaired 2-tailed *t* test was used to make comparisons between two groups and one-way analysis of variance (ANOVA) with Tukey's correction or Kruskal−Walls nonparametric test followed by Dunn's test was used to make multiple comparisons between the groups. A P value < 0.05 was defined as statistical significance.

2.8. Data and resource availability

Sequencing data for *Ddah1*$^{f/f}$ fed with HFD and *Ddah1*^{HKO} or HFD-WT and DDAH1-TG mice were deposited in the NCBI Sequence Read Archive database (http://www.ncbi.nlm.nih.gov/bioproject/768483). Other data sets generated and/or analyzed during the current study are available from the corresponding author upon reasonable request.

3. Results

3.1. Hepatocyte-specific Ddah1 deficiency exacerbated liver dysfunction and insulin resistance in HFD-fed mice

The inducible *Ddah1*^{HKO} mice was generated using the strategy illustrated in Fig. 1A. Western blot analysis demonstrates that DDAH1 expression was undetectable in primary hepatocytes isolated from adult *Ddah1*^{HKO} mice (Fig. 1B). To determine the effect of hepatocellular deletion of *Ddah1* on hepatic steatosis, male *Ddah1*^{HKO} mice and *Ddah1*$^{f/f}$ were fed a RC or HFD for 16 weeks. During the period of RC or HFD feeding, the body weight was not different between the *Ddah1*^{HKO} and *Ddah1*$^{f/f}$ mice (Supporting Information Fig. S1A). In RC-fed mice, hepatocyte-specific *Ddah1* deletion significantly increased serum ADMA and ALT levels (Fig. 1C and D). HFD feeding for 16 weeks caused significantly higher serum levels of ADMA, AST, ALT and leptin in the *Ddah1*^{HKO} mice than in the *Ddah1*$^{f/f}$ mice (Fig. 1C−F), indicating that *Ddah1*^{HKO} exacerbated HFD-induced liver dysfunction. There were no significant differences in liver weight, the ratio of liver weight to body weight and serum TG and total cholesterol (TC) between *Ddah1*$^{f/f}$ and *Ddah1*^{HKO} mice after HFD feeding (Fig. 1G, H, and Fig. S1B and S1C). In RC-fed mice, *Ddah1*^{HKO} had no effect on fasting blood glucose or insulin levels. HFD feeding increased fasted blood glucose and serum insulin levels in both groups. However, obese *Ddah1*^{HKO} mice exhibited higher fasting blood glucose and serum insulin levels than obese *Ddah1*$^{f/f}$ mice (Fig. 1I and J). As indicated by delayed glucose clearance and increased area under the curve (AUC) in OGTT, glucose tolerance was impaired in HFD-fed mice, and this impairment was significantly more severe in *Ddah1*^{HKO} mice than in *Ddah1*$^{f/f}$ mice (Fig. 1K). ITT results show that insulin sensitivity was decreased in HFD-fed mice and *Ddah1*^{HKO} mice were less insulin-sensitive than diet-matched *Ddah1*$^{f/f}$ mice (Fig. 1L).

3.2. Hepatocyte-specific Ddah1 deficiency exacerbated hepatic steatosis and oxidative stress in HFD-fed mice

In response to RC feeding, *Ddah1*^{HKO} slightly increased liver ADMA levels and had no obvious effect on liver TG, TC or 4-hydroxynonenal (4-HNE) levels. HFD feeding caused significantly higher liver ADMA, TG and 4-HNE levels in the *Ddah1*^{HKO} mice than in the *Ddah1*$^{f/f}$ mice (Fig. 2A−D). Histopathological analysis of liver sections using H&E, Oil Red O, and dihydroethidium (DHE) staining demonstrated that more severe hepatic steatosis and oxidative stress were observed in the livers of HFD-fed *Ddah1*^{HKO} mice than in similar-fed *Ddah1*$^{f/f}$ mice (Fig. 2E). As revealed by the qPCR results, HFD feeding significantly increased the mRNA levels of *Srebp1c*, *Fasn*, *Cd36*, *Fgf21*, *Pparγ*, *Cidea* and *Cidec*. However, the up-regulation of these genes was exacerbated in the livers of *Ddah1*^{HKO} mice (Fig. 2F). Consistently, HFD feeding resulted in increased protein expression of FAS, CD36, PPARγ and CIDEA in the livers of *Ddah1*^{HKO} mice. As expected, DDAH1 expression was significantly decreased in the livers of *Ddah1*^{HKO} mice. HFD feeding significantly increased DDAH1 expression in the livers of both genotypes. DDAH2 expression was not affected by *Ddah1*^{HKO} and HFD (Fig. 2G).

3.3. Global overexpression of DDAH1 improved insulin resistance, hepatic steatosis and oxidative stress in HFD-fed mice

To confirm that DDAH1 can protect against insulin resistance and hepatic steatosis in HFD-fed mice, male DDAH1-TG mice and their littermate wild type controls (WT) were fed an HFD for 16 weeks. At the end of the experimental period, DDAH1-TG mice exhibited significantly lower serum ADMA levels than diet-matched WT mice (Fig. 3A). DDAH1 overexpression significantly decreased body weight, liver weight, ratio of liver weight to body weight and serum TG, TC, ALT, AST and leptin levels

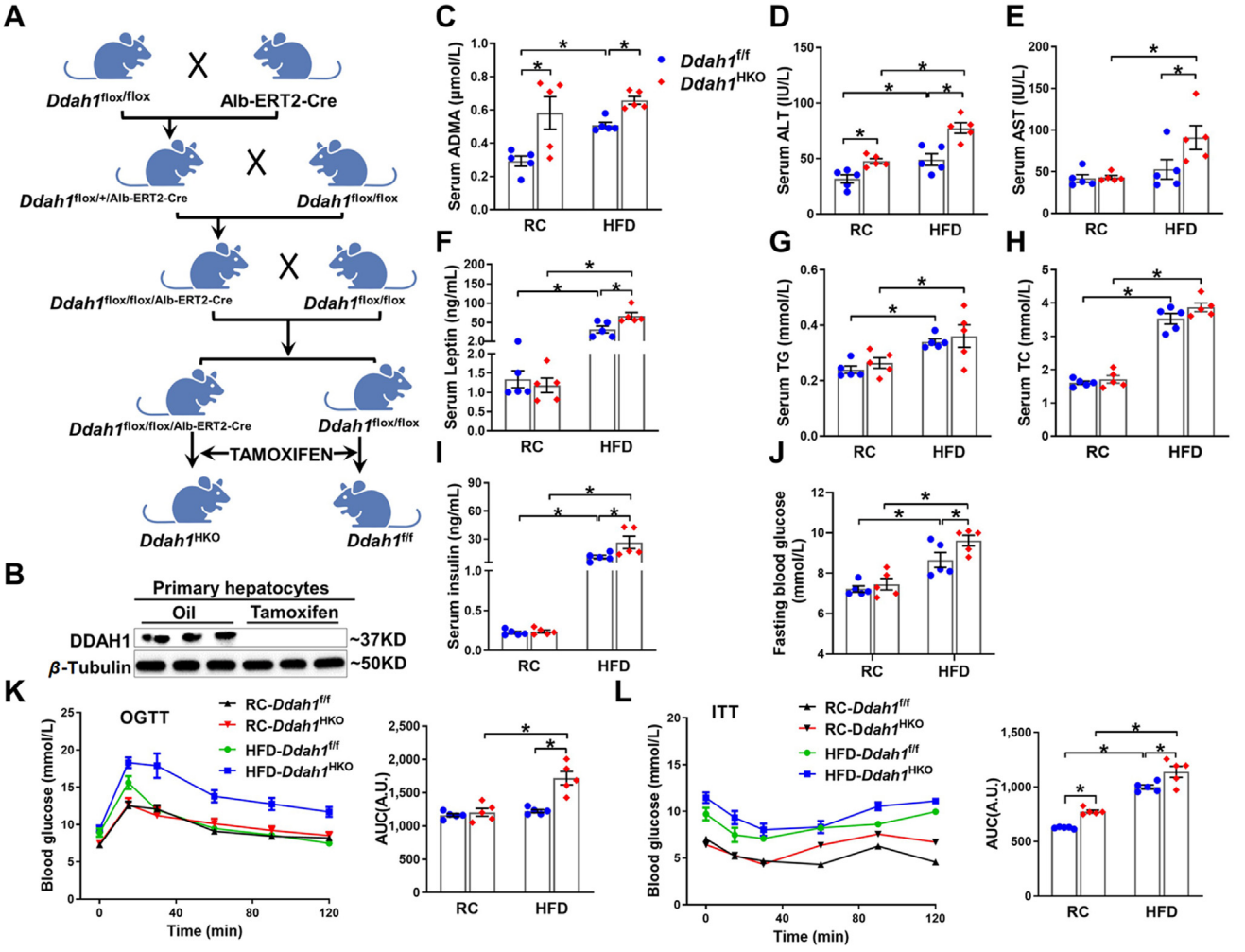

Figure 1 Hepatocyte-specific deletion of *Ddah1* exacerbated high-fat diet-induced liver dysfunction and insulin resistance. (A) The diagram shows the approach for generating the *Ddah1*^{HKO} mice. (B) Western blot shows diminished DDAH1 expression in isolated primary hepatocytes. (C–J) Male *Ddah1*^{HKO} and *Ddah1*$^{f/f}$ mice were fed a RC or an HFD for 16 weeks. Serum ADMA (C), ALT (D), AST (E), leptin (F), TG (G), TC (H), fasting blood glucose (I) and serum insulin levels (J) levels were measured. (K, L) OGTT (K) and ITT (L) were performed and the corresponding AUCs of blood glucose levels in each group were calculated. Data are mean ± SEM, $n = 5$; $^*P < 0.05$. A.U., arbitrary unit.

(Fig. 3B–F, and Supporting Information Fig. S2A–S2C). After HFD feeding, DDAH1-TG mice also exhibited lower fasting blood glucose and insulin levels than obese WT mice (Fig. 3G and H). OGTT and ITTs also showed that DDAH1 overexpression attenuated HFD-induced impairments in glucose excretion capacity and insulin sensitivity (Fig. 3I and J).

In RC-fed mice, DDAH1 overexpression had no noticeable effect on liver TG and TC levels. HFD feeding resulted in significantly lower liver TG, TC and 4-HNE levels in DDAH1-TG mice than in WT mice (Fig. 3K, L, and Fig. S2D). Furthermore, H&E, Oil Red O and DHE staining demonstrated that DDAH1 overexpression resulted in less hepatic steatosis and superoxide production in the livers of HFD-fed mice (Fig. 3M). DDAH1 overexpression also attenuated the increases in FAS, CD36, PPARγ and CIDEA protein expression in the livers of HFD-fed mice (Fig. 3M). HFD feeding significantly increased hepatic DDAH1 expression in both genotypes, and DDAH1-TG mice exhibited higher hepatic DDAH1 expression than diet-matched WT mice (Fig. 3N).

3.4. Hepatocyte-specific overexpression of DDAH1 alleviated insulin resistance, hepatic steatosis and oxidative stress in ob/ob mice

To further confirm that hepatocyte-specific overexpression of DDAH1 could alleviate NAFLD, we treated *ob/ob* mice with AAV8-DDAH1 by tail vein injection. Mice that received AAV8-His by injection were used as controls. The experimental processes are illustrated in Supporting Information Fig. S3A. DDAH1 overexpression in hepatocytes decreased serum levels of ADMA, AST, ALT, TG, TC and insulin, and blood glucose levels (Fig. 4A–E, and Supporting Information Fig. S3). DDAH1 overexpression also decreased liver TG, TC, 4-HNE and 3′-NT levels in *ob/ob* mice (Fig. 4F–J). The results of OGTT and ITT reveal that DDAH1 overexpression did not affect glucose excretion but increased insulin sensitivity in *ob/ob* mice (Fig. 4K and L). Histopathological analysis of liver sections showed that liver injury, hepatic steatosis and superoxide generation in *ob/ob* mice were ameliorated by DDAH1 overexpression (Fig. 4M). Western

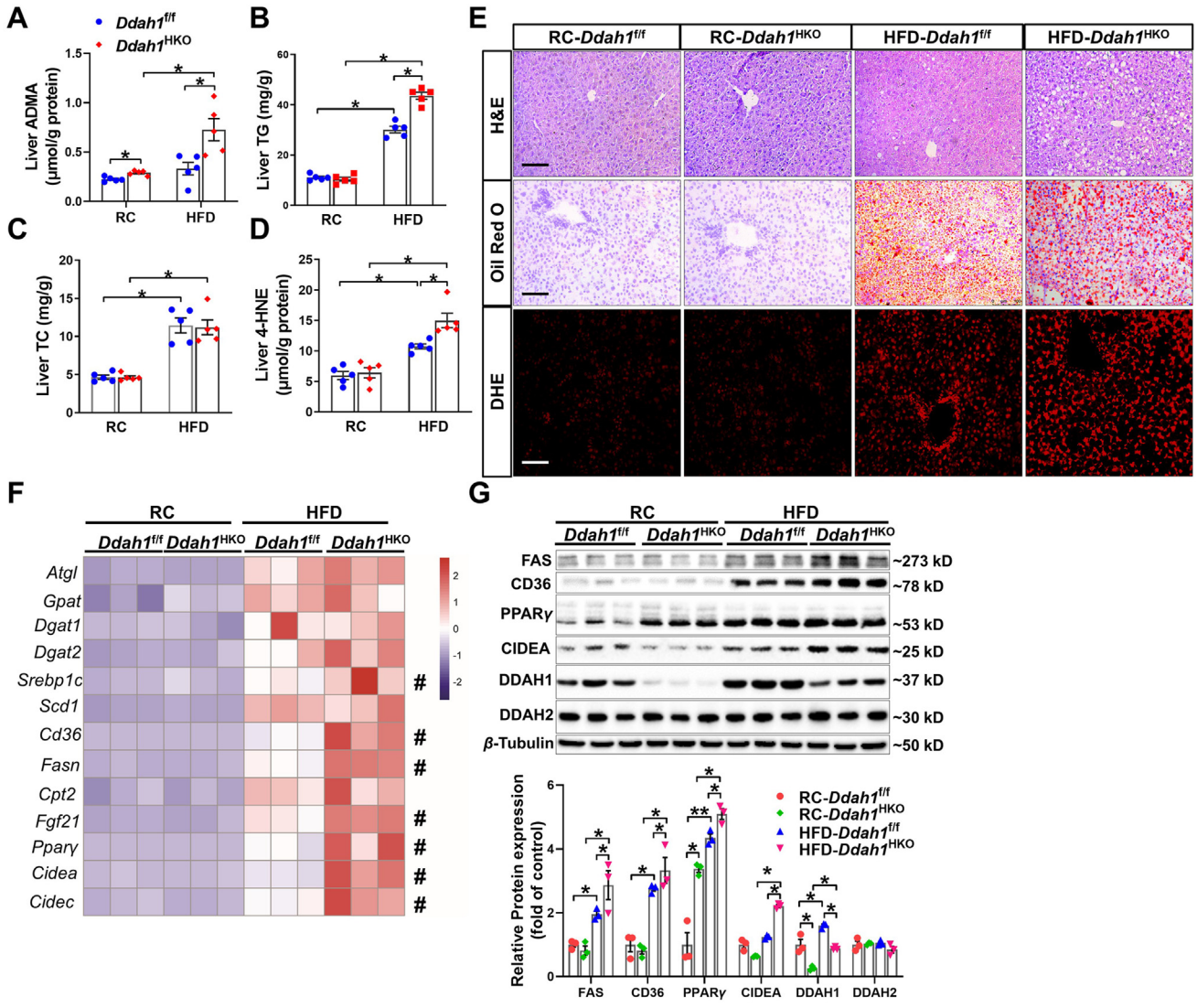

Figure 2 Hepatic *Ddah1* deficiency aggravated hepatic steatosis and oxidative stress in HFD-fed mice. (A−D) The levels of ADMA (A), TG (B), TC (C) and 4HNE (D) in the liver were measured. (E) Representative liver sections were stained with H&E (upper panel), Oil Red O (middle panel) and DHE (lower panel). Scale bar = 100 μm. (F) The mRNA levels of lipid metabolic genes were measured by real-time qPCR, and the gene expression profiles are shown in the heat map. # indicates the difference between HFD- *Ddah1*$^{f/f}$ and HFD-*Ddah1*^{HKO} was significant. (G) Liver lysates were examined by Western blot, and proteins were normalized to β-Tubulin. In (A)−(D), $n = 5$; in (F) and (G), $n = 3$; data are presented as the mean ± SEM; $^{*}P < 0.05$; $^{**}P < 0.01$.

blot analysis demonstrated that AAV8-DDAH1 injection increased hepatic DDAH1 expression by ∼60% and significantly decreased the protein expression of FAS, CD36, PPARγ and CIDEA (Fig. 4N).

3.5. *DDAH1 regulates NF-κB signaling, lipid metabolic process, and immune system process in the livers of obese mice*

To investigate the molecular mechanism by which DDAH1 protects against NAFLD in mice, we performed microarray or RNA sequencing to analyze the changes in the whole-genome expression profile of fatty livers. We identified 306 DEGs between the HFD-fed *Ddah1*$^{-/-}$ *and* WT groups, 609 DEGs between the HFD-fed DDAH1-Tg and WT groups and 662 DEGs between the HFD-fed *Ddah1*^{HKO} *and Ddah1*$^{f/f}$ groups. A Venn diagram showed that there were 29 overlapping DEGs in the three groups (Fig. 5A), and the expression profiles of these 29 overlapping DEGs in the three groups are shown in the heat map (Fig. 5B). We performed KEGG pathway enrichment analysis using the Database for Annotation, Visualization and Integrated Discovery (https://david.ncifcrf.gov/) and identified 12 genes that were significantly enriched in NF-κB signaling, lipid metabolic process and immune system process pathways (Fig. 5C). We also performed real-time qPCR to validate the changes in these genes in fatty livers and found that these genes were significantly up-regulated by hepatocyte specific deletion of *Ddah1* in but downregulated by overexpression of DDAH1 (Fig. 5D and Supporting Information Fig. S4).

To determine the effect of DDAH1 on NF-κB signaling, we measured the protein expression of total and phosphorylated p65 and IκBα. The results of Western blot reveal that HFD increased the ratios of p-p65 (Ser536) to total p65 and p-IκBα (Ser32) to

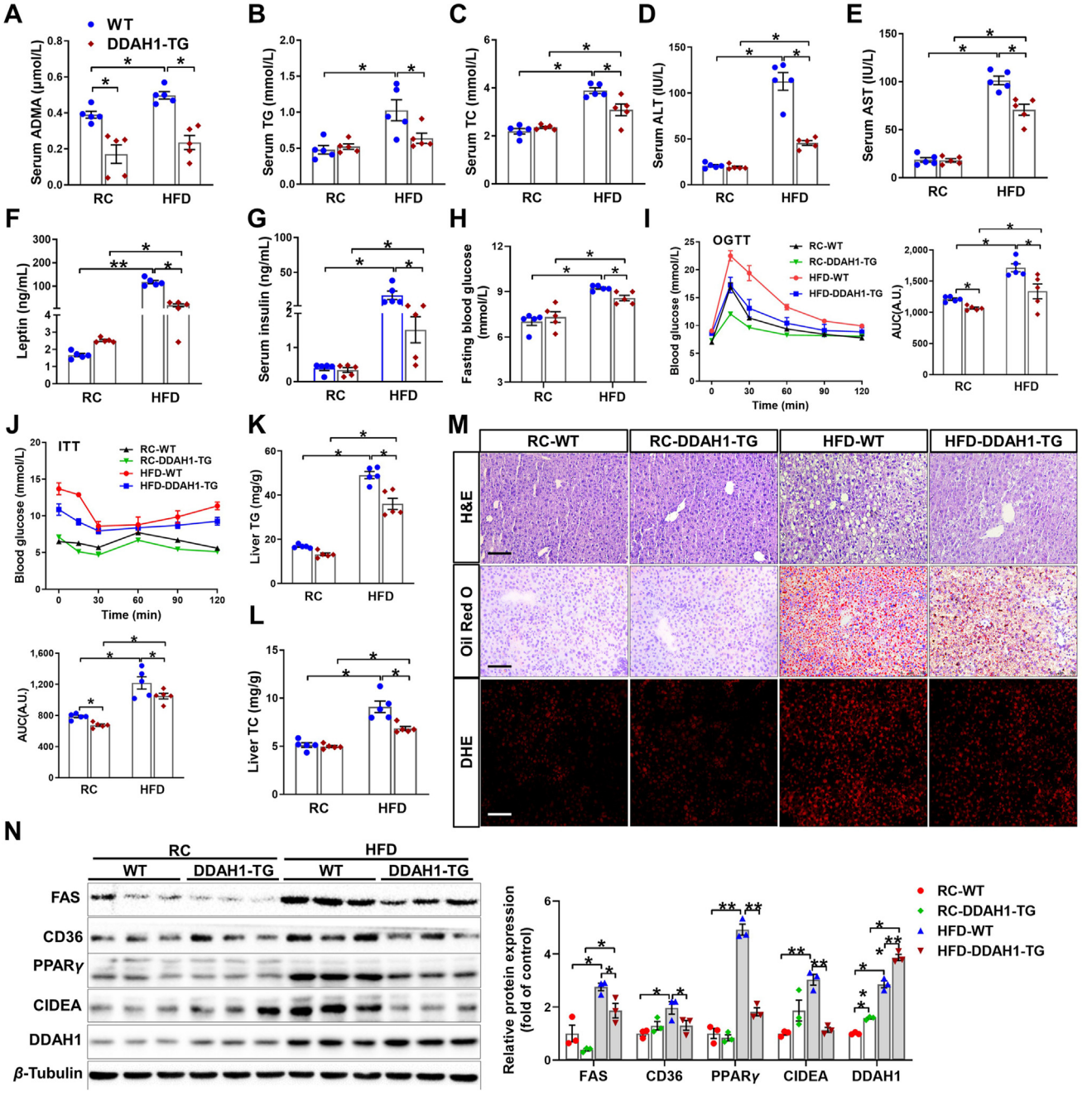

Figure 3 Global overexpression of DDAH1 alleviated liver dysfunction, hepatic steatosis, insulin resistance and oxidative stress in HFD-fed mice. (A−H) After RC or HFD feeding for 16 weeks, the serum ADMA (A), TG (B), TC (C), ALT (D), AST (E), leptin (F), insulin (G) and fasting blood glucose (H) levels of RC- or HFD-fed DDAH1-TG and WT littermates were measured. (I, J) OGTT (I) and ITTs (J) were performed and the corresponding AUC in each group were calculated. (K, L) The liver TG (K) and TC (L) levels were measured. (M) Representative liver sections were stained with H&E, Oil Red O, and DHE. Scale bar = 100 μm. (N) Liver lysates were examined by Western blot. In (A)−(L), $n = 5$; in (N), $n = 3$; data are mean ± SEM; $^{*}P < 0.05$; $^{**}P < 0.01$.

total IκBα ratios, and these increases were exacerbated in the livers of HFD-fed *Ddah1*^{HKO} mice, but attenuated in the livers of HFD-fed DDAH1-TG mice. The ratios of p-JNK (Thr183/Tyr185) to total JNK were also increased in fatty livers. However, JNK activation was exacerbated by hepatocyte specific deletion of *Ddah1* but attenuated by overexpression of DDAH1 (Fig. 5E and Supporting Information Fig. S5). Furthermore, HFD-induced upregulation of S100A11, MOGAT2, VLDLR, APOA4 and CIDEC were exacerbated in the livers of *Ddah1*^{HKO} mice (Fig. 5E).

3.6. DDAH1 regulates S100A11 via NF-κB, JNK and oxidative stress-dependent manner in hepatocytes

To investigate whether the upregulated genes related to lipid metabolism also affect DDAH1 expression, we overexpressed

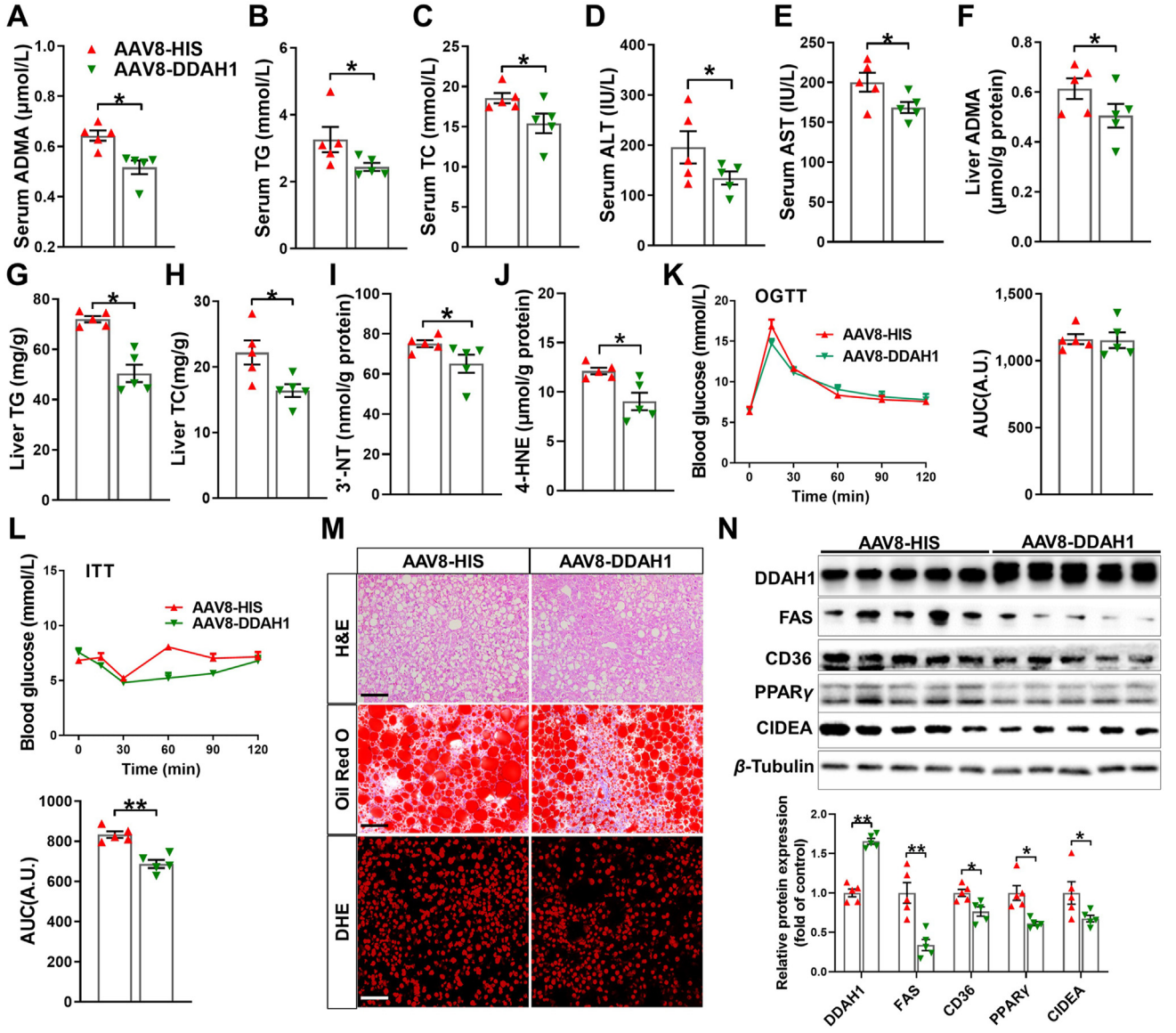

Figure 4 DDAH1 overexpression improved hepatic steatosis and oxidative stress in *ob*/*ob* mice. (A−E) *ob*/*ob* mice were treated with AAV8-HIS or AAV8-DDAH1 by tail vein injection. At 4 weeks after injection, the mice were sacrificed and serum ADMA (A), TG (B), TC (C), ALT (D) and AST (E) were measured. (F−J) Liver ADMA (F), TG (G), TC (H), 3′-NT (I) and 4-HNE (J) levels were measured. (K, L) OGTTs and ITTs were performed in *ob*/*ob* mice treated with AAV8-HIS and rAAV8-DDAH1 and the corresponding AUCs for blood glucose levels in each group were calculated. (M) Representative liver sections were stained with H&E, Oil Red O and DHE. Scale bar = 100 μm. (N) Liver lysates were examined by Western blot analysis. Data are mean ± SEM, $n = 5$; *$P < 0.05$; **$P < 0.01$.

these genes in HepG2 cells by transfecting the corresponding expression vector. VLDLR, CIDEC, and APOA4 did not affect DDAH1 expression, while S100A11 overexpression dramatically decreased endogenous DDAH1 expression (Fig. 6A and Supporting Information Fig. S6). Although MOGAT2 overexpression also decreased DDAH1 expression by ∼12%, the difference was not statistically significant. Additionally, the depletion of S100A11 increased the expression of DDAH1 in PA-treated HepG2 cells (Fig. 6B).

S100A11 is known as an inducer of inflammatory processes in the development of hepatocellular carcinoma[20]; therefore, it could be regulated by NF-κB. The search in the online database (https://jaspar.genereg.net/) suggested that there is a putative NF-κB binding site (−322 to −312 bp) in the promoter of S100A11. To determine the regulatory effect of NF-κB on S100A11, we generated three reporter constructs driven by different regions of the S100A11 promoter. Cotransfection of NF-κB/p65 plasmid and the reporter construct driven by the 2000 bp or 398 bp promoter of S100A11 in HEK293 cells significantly increased the luciferase activity. However, NF-κB/p65 could not increase luciferase activity when the reporter construct was driven by 313 bp of the S100A11 promoter (Fig. 6C), indicating that the putative binding site is essential for the transcriptional regulation of S100A11 by NF-κB.

The enzyme activity of human DDAH1 has been reported to be completely diminished when His^{173} or Cys^{274} was mutated to alanine[21]. Therefore, we generated a H173A/C274A mutation of DDAH1. DDAH1 overexpression significantly decreased S100A11 promoter luciferase activity in p65-transfected HEK293

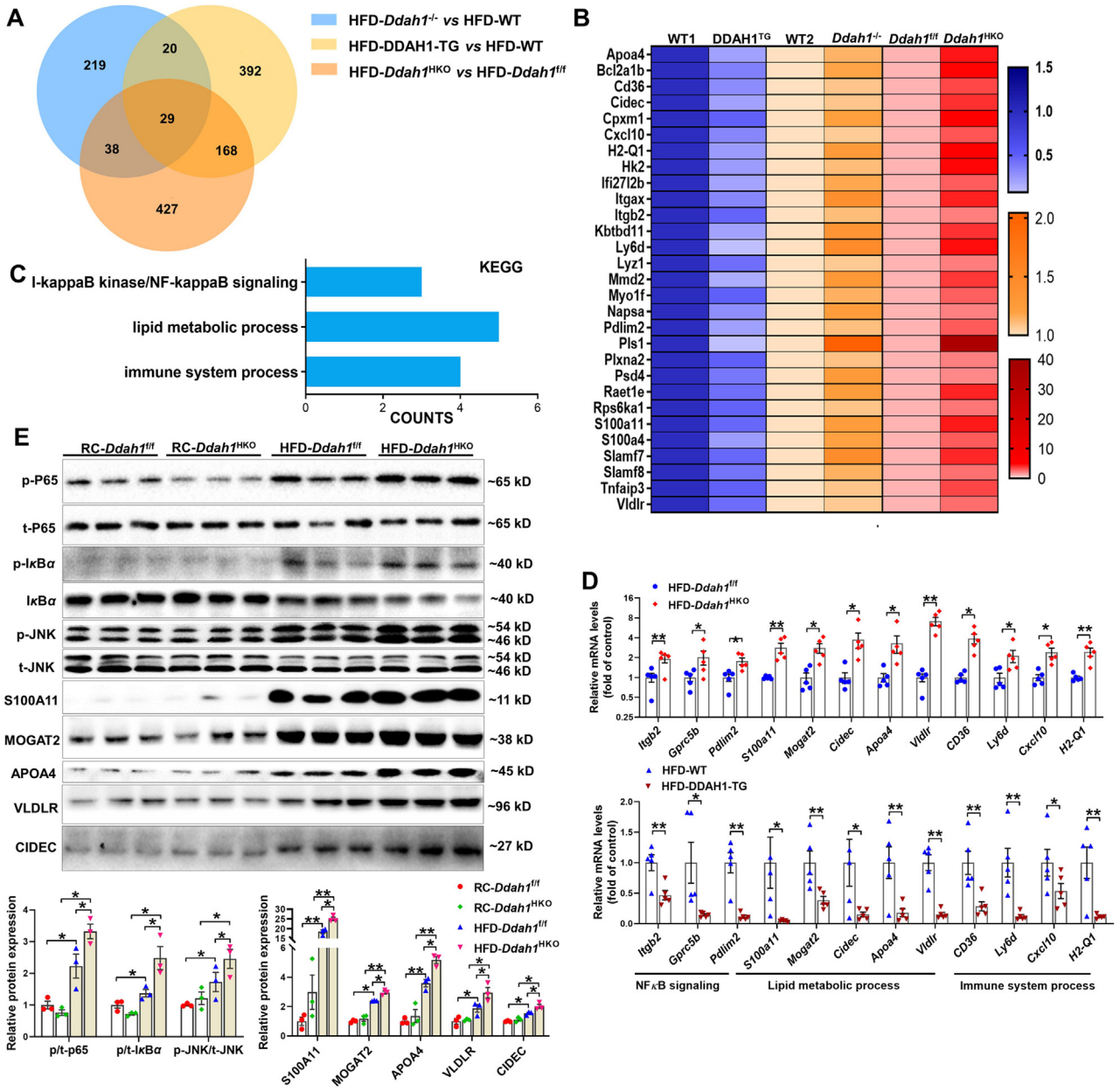

Figure 5 DDAH1 regulated multiple pathways in the fatty liver. (A) Venn diagram shows the number of DEGs and overlapping DEGs from the HFD-WT *vs*. HFD-*Ddah1*$^{-/-}$, HFD-WT *vs*. HFD-DDAH1-TG and HFD-*Ddah1*$^{f/f}$ *vs*. HFD-*Ddah1*^{HKO} groups. (B) Heat map of gene expression of the overlapping DEGs. (C) KEGG analysis of the overlap DEGs from the HFD-WT *vs*. HFD-*Ddah1*$^{-/-}$, HFD-WT *vs*. HFD-DDAH1-TG and HFD-*Ddah1*$^{f/f}$ *vs*. HFD-*Ddah1*^{HKO} groups. Gene counts are displayed on the *x*-axis, and enriched KEGG pathways are displayed on the *y*-axis. (D) The mRNA levels of the genes involved in the enriched KEGG pathway in the livers of HFD-fed *Ddah1*$^{f/f}$ and *Ddah1*^{HKO} or WT and DDAH1-TG mice were measured by qPCR. (E) Liver lysates of RC- and HFD-fed *Ddah1*$^{f/f}$ and *Ddah1*^{HKO} mice were examined by Western blotting. In (D), $n = 5$; in (E), $n = 3$; data are the mean ± SEM; $^{*}P < 0.05$; $^{**}P < 0.01$.

cells, and this reduction was attenuated by the H173A/C274A mutation (Fig. 6D). On the other hand, DDAH1 depletion also increased S100A11 promoter luciferase activity in both BSA- and PA-treated HepG2 cells (Fig. 6E). DDAH1 overexpression decreased S100A11 expression in PA-treated HepG2 cells while overexpression of DDAH1(H173A/C274A) mutation had less effect on the reduction of S100A11 (Fig. 6F). Furthermore, overexpression of DDAH1 also decreased the expression of S100A11 in the livers of HFD-fed mice or *ob*/*ob* mice (Fig. 6G).

To further investigate the mechanism by which DDAH1 regulates S100A11 in fatty livers, we used primary WT and *Ddah1*$^{-/-}$ hepatocyte as cell models. After PA treatment, *Ddah1* deficiency increased S100A11 expression and phosphorylation of p65 and JNK in primary hepatocytes. *Ddah1* deficiency also increased the nuclear p65 (n-p65) content in PA-treated primary hepatocytes (Fig. 6H). To further determine whether NF-κB, JNK and oxidative stress are involved in the regulating S100A11 by DDAH1 in primary hepatocytes, we incubated the PA-treated *Ddah1*$^{-/-}$ hepatocytes with

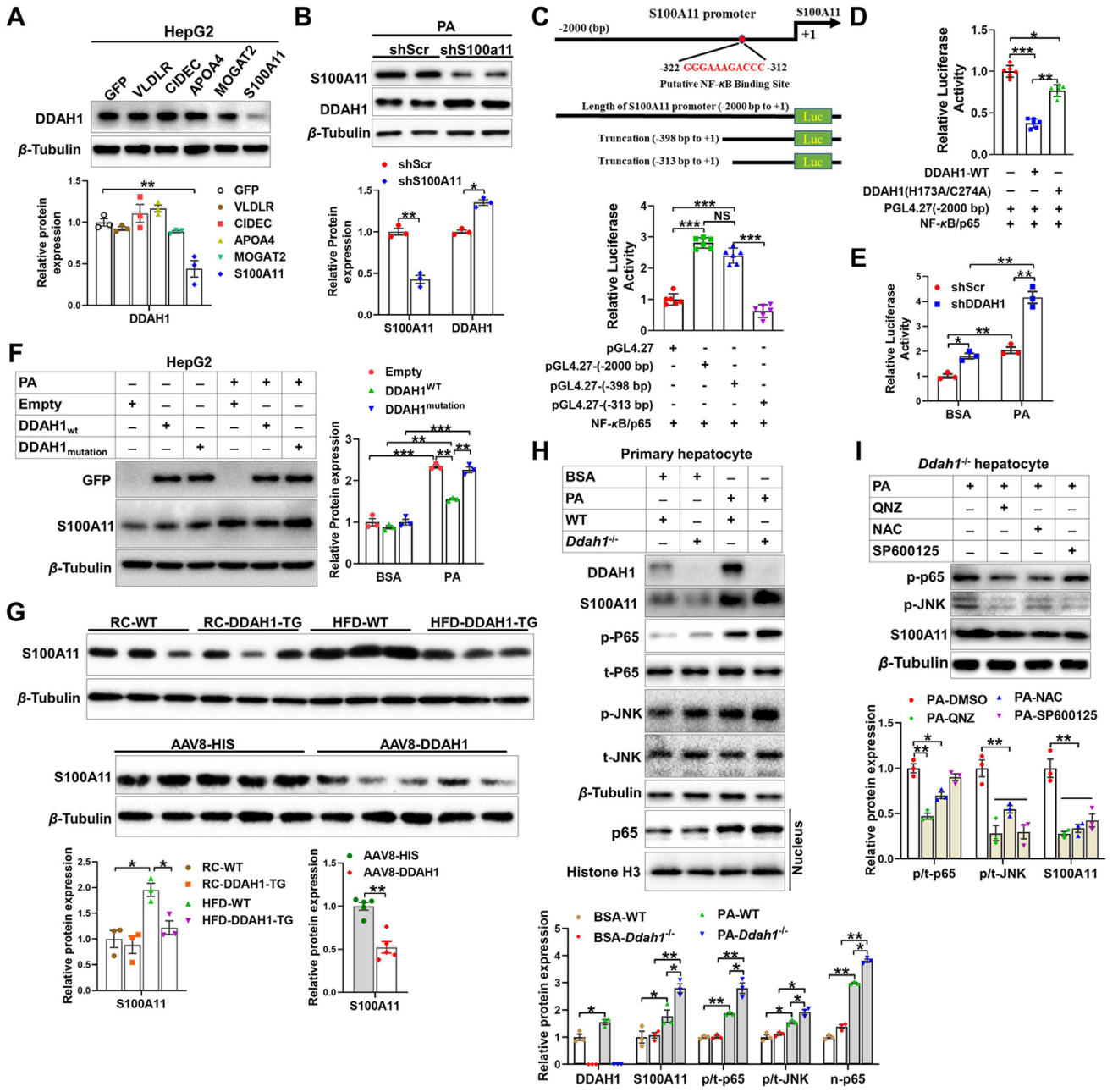

Figure 6 DDAH1 regulated the expression of S100A11 in fatty livers and hepatocytes. (A) HepG2 cells were transfected with pCMV3-ORF constructs and then cell lysates were examined by Western blotting. (B) HepG2 cells were transfected with shS100A11 or shRNA targeting a scrambled sequence (shScr) lentiviral vector, and then incubated with 0.5 mmol/L PA for 48 h. Cell lysates were examined by Western blot. (C) The structures of the S100A11 promoter reporter constructs and the putative NF-κB binding site are illustrated in the diagram. HEK293 cells were cotransfected with NF-κB/p65 plasmid and the reporter construct, and then luciferase activity was measured. (D) Luciferase activity was measured in HEK293 cells transfected with the S100A11 promoter reporter construct, p65, and human DDAH1 or its mutation. (E) After incubation with BSA or 0.5 mmol/L PA for 24 h, the S100A11 promoter luciferase activity was measured in HepG2 cells transfected with shDDAH1 or shScr lentiviral vectors. (F) HepG2 cells transfected with empty, GFP-tagged WT or mutated DDAH1 retroviral vectors were incubated with 0.25 mmol/L PA for 48 h and then cell lysates were examined by Western blot. (G) The expression of S100A11 in the livers from different groups was determined by Western blotting. (H) BSA or 0.25 mmol/L PA treated WT and *Ddah1*$^{-/-}$ primary hepatocytes were examined by Western blot. The 'n-p65' refers to nuclear p65. (I) Primary *Ddah1*$^{-/-}$ hepatocytes were treated with 0.25 mmol/L PA plus 50 nmol/L QNZ, 5 mmol/L NAC, or 50 nmol/L SP600125 for 24 h and cell lysates were examined by Western blot. In (A), (B), (E), (F), (H) and (I), $n = 3$; in (C) and (D), $n = 6$; in (G), $n = 3$ or 5; data are mean ± SEM; $^{*}P < 0.05$, $^{**}P < 0.01$, $^{***}P < 0.001$.

NF-κB inhibitor QNZ, broad spectrum JNK inhibitor SP600125 and antioxidant NAC. As shown in Fig. 6I, QNZ and NAC significantly decreased phosphorylated p65 and JNK and S100A11 expression in PA-treated *Ddah1*$^{-/-}$ hepatocytes. SP600125 decreased p-JNK levels and S100A11 expression, but had no significant effect on p-p65 levels (Fig. 6I). QNZ, NAC, and SP600125 also significantly

decreased the protein expression of MOGAT2, VLDLR, APOA4, and CIDEC (Supporting Information Fig. S7).

Interestingly, ADMA increased the expression of S100A11 by ~20% in HepG2 cells and this increase was further enhanced by PA treatment. ADMA did not affect DDAH1 expression. However, PA caused a significant reduction in DDAH1 expression in the presence of exogenous ADMA (Supporting Information Fig. S8).

We also examined the protein expression of DDAH1 and S100A11 in the livers of mice fed with HFD for different time. HFD feeding for 10 weeks significantly increased hepatic DDAH1 and S100A11 expression. HFD feeding for another 10 weeks further increased S100A11 expression whereas decreased DDAH1 expression (Supporting Information Fig. S9).

3.7. *Knockdown of S100a11 alleviates hepatic steatosis, insulin resistance, and oxidative stress in HFD-fed Ddah1^{HKO} mice*

To confirm that S100A11 participates in the regulatory effect of DDAH1 on lipid metabolism, we depleted *S100a11* from the livers of HFD-fed mice *via* tail vein injection of the AAV8-sh*S100a11* vector. AAV8-GFP was used as control (Fig. 7A). As revealed by Western blot, AAV8-sh*S100a11* decreased hepatic S100A11 expression by approximately 50%. *S100a11* knockdown increased hepatic DDAH1 expression in the HFD-fed *Ddah1*$^{f/f}$ and *Ddah1*^{HKO} mice (Fig. 7B). Knockdown of *S100a11* also resulted in significant decreases in serum ALT and AST levels in HFD-fed *Ddah1*^{HKO} mice and the differences in those values between HFD-fed *Ddah1*$^{f/f}$ and *Ddah1*^{HKO} mice were diminished (Fig. 7C and D). After *S100a11* knockdown, the glucose tolerance and insulin sensitivity were improved in HFD-fed *Ddah1*^{HKO} mice (Fig. 7E and F). Histopathological staining demonstrated that the pathological abnormalities, steatosis and superoxide generation in the livers of HFD-fed mice were ameliorated by *S100a11* knockdown (Fig. 7G and Supporting Information Fig. S10). In the livers of HFD-fed mice, *S100a11* knockdown decreased TG levels and abolished the hepatic *Ddah1* deficiency-mediated increases in TG levels (Fig. 7H). *S100a11* knockdown resulted in significant decreases in TC and 4-HNE levels in the livers of HFD-fed *Ddah1*^{HKO} mice (Fig. 7I and J). After *S100a11* knockdown, there were no significant differences in protein expression of FAS, CIDEA, CIDEC, CD36, PPARγ and p-p65 between HFD-fed *Ddah1*$^{f/f}$ and *Ddah1*^{HKO} mice, and hepatic p-JNK expression was lower in HFD-fed *Ddah1*^{HKO} mice than in HFD-fed *Ddah1*$^{f/f}$ mice (Fig. 7K).

We also transfected HepG2 cells with the sh*S100A11* vector. As monitored by Nile Red and CellROX deep red staining, the knockdown of S100A11 significantly attenuated lipid accumulation and oxidative stress in PA-treated cells. However, there was still a significant difference in the Nile Red fluorescence intensity between DDAH1-depleted and control cells. Western blot results showed that knockdown of S100A11 significantly attenuated PA-induced upregulation of FAS, CIDEA, CIDEC and phosphorylation of NF-κB p65 in DDAH1-depleted cells (Supporting Information Fig. S11).

4. Discussion

This study presents two major new findings. First, we demonstrated that hepatic DDAH1 could protect against hepatic steatosis and IR in obese mice and that the underlying mechanism was associated with the degradation of ADMA and the inhibition of lipogenesis and inflammation. Second, we identified DDAH1 as a novel regulator of S100A11 in the fatty liver that could provide novel insights into the pathogenesis of NAFLD.

As a critical enzyme for the degradation of ADMA, global deletion or overexpression of DDAH1 profoundly affects ADMA levels. However, DDAH1 is differently expressed in different tissues, and the tissue/cell-specific role of DDAH1 in circulating ADMA levels remains unclear. Previous reports have shown that vascular endothelial-specific *Ddah1* deficiency significantly increases plasma ADMA level[14], while cardiomyocyte- or proximal tubule-specific *Ddah1* KO does not affect plasma ADMA levels[22,23]. Here, we showed that hepatocyte-specific *Ddah1* deletion caused significant increases in serum ADMA levels. Since insulin-mediated tissue glucose uptake is NO-dependent, it is likely that increased circulating ADMA levels may promote whole-body IR in metabolic diseases by decreasing NO production. In fact, increased plasma ADMA levels in patients with NAFLD are associated with IR[8]. In this regard, hepatic DDAH1 may enhance insulin sensitivity in obese mice by decreasing serum ADMA levels.

Under some pathological conditions, ADMA can promote ROS production by acting as a substrate for uncoupled eNOS[24], activating NADPH oxidase[25] or upregulating the renin-angiotensin system[25]. In HepG2 cells, ADMA administration has been found to increase intracellular ROS and TG levels[13]. Interestingly, here we found that ADMA increased S100A11 expression and even promoted the down-regulation of DDAH1 in PA-treated cells. Therefore, accelerated ADMA accumulation in the fatty liver could decrease NO bioavailability, repress DDAH1 expression, increase oxidative stress and upregulate S100A11 expression. The protective effects of liver DDAH1 against the development of NAFLD were also due, at least in part, to attenuating ADMA accumulation in the fatty liver, which could contribute to the transition from steatosis to steatohepatitis.

Hepatic lipid accumulation may be induced by increased lipid uptake and *de novo* fatty acid synthesis, impaired hepatic β-oxidation and decreased hepatic lipid export[26,27]. In the present study, hepatic *Ddah1* deficiency exacerbated the upregulation of *Ppar*γ and *Srebp1c*, two important transcription factors for lipid metabolism[28,29], as well as their downstream target genes (*Cidea*, *Cidec*, *Fasn*, *Cd36*, *Apoa4* and *Vldlr*) in fatty livers, suggesting a potential mechanism for the DDAH1-dependent regulation of lipid accumulation in fatty livers. DDAH1 may also attenuate lipid accumulation by suppressing *Cpxm1*, a positive regulator of adipogenesis[30], and *Mogat2*, a rate-limiting acyltransferase[31].

The most interesting implication of the present study is the identification of DDAH1 as a novel regulator of S100A11, which was recently identified as an important regulator of lipid metabolism[32,33]. S100A11 was originally found to be upregulated with inflammation and fibrosis in the liver and further increased drastically in mouse/human hepatocellular carcinoma and intrahepatic cholangiocarcinoma[20,34]. Recently, two independent reports demonstrated that S100A11 is up-regulated in the livers of NAFLD patients and obese mice, and overexpression of S100A11 can promote liver steatosis[32,33]. In agreement with those reports, we also found that S100A11 was upregulated in fatty livers and PA-treated cells and that this upregulation was regulated by hepatic DDAH1 at the transcriptional level. The present study also showed that knockdown of *S100a11* attenuated TG accumulation,

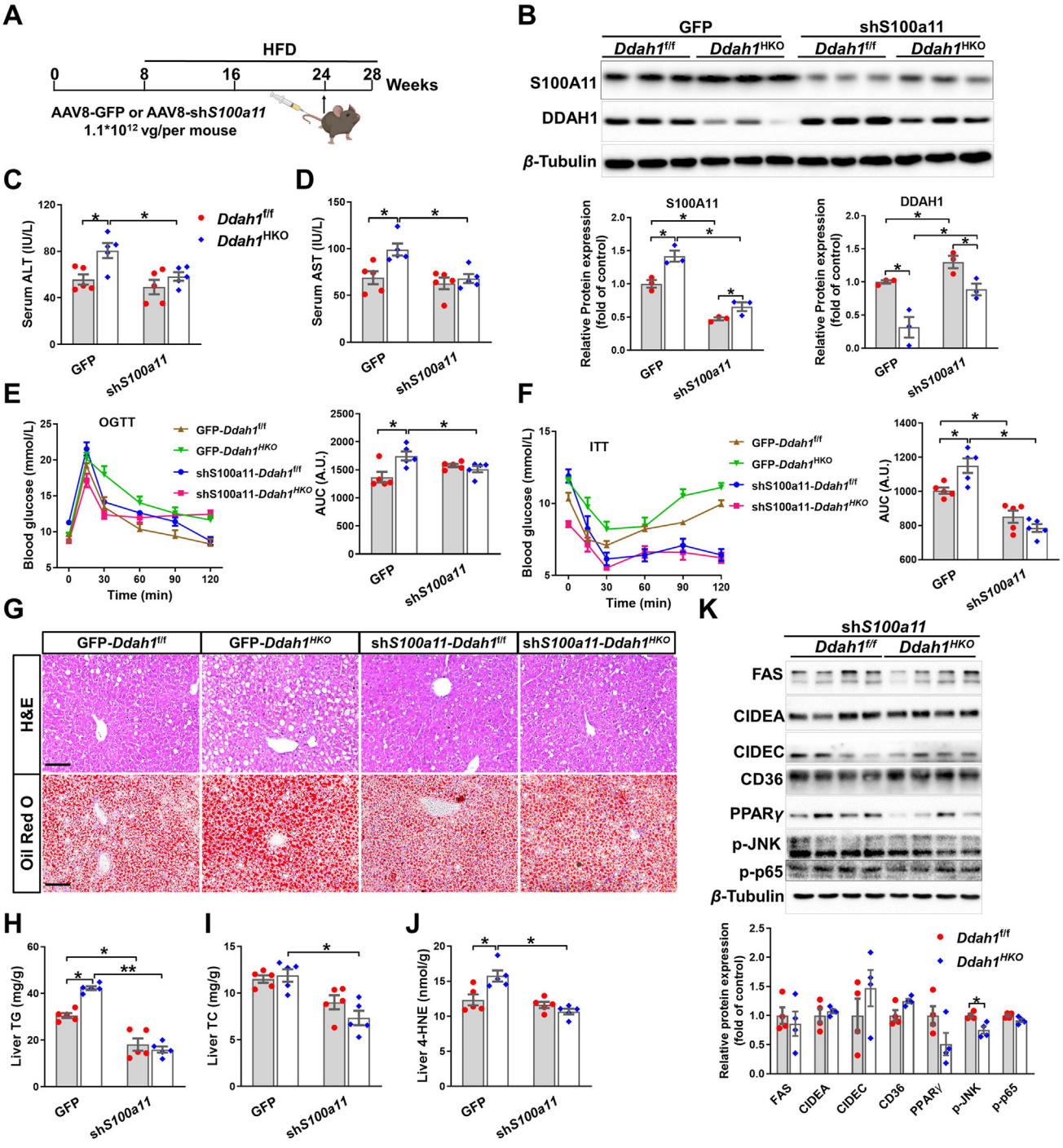

Figure 7 *S100a11* knockdown ameliorated insulin resistance and hepatic steatosis in HFD-fed *Ddah1*^{HKO} mice. (A) After HFD feeding for 16 weeks, *Ddah1*$^{f/f}$ and *Ddah1*^{HKO} mice were treated with AAV8-GFP or AAV8-shS100a11 *via* tail vein injection. The timeline of the experimental process was illustrated in the diagram. (B) Liver lysates were examined by Western blots for the expression of DDAH1 and S100A11. (C, D) Serum ALT and AST levels were measured. (E, F) OGTT and ITT were performed on GFP- and sh*S100a11*-treated mice, and the corresponding AUCs for blood glucose levels in each group were calculated. (G) Representative liver sections were stained with H&E and Oil Red O. Scale bar = 100 μm. (H–J) Liver TG (H), TC (I), and 4-HNE (J) levels were measured. (K) Liver lysates were examined by Western blot analysis. In (B), $n = 3$; in (C)–(J), $n = 5$; in (K), $n = 4$. Data are represented as mean ± SEM; $^{*}P < 0.05$, $^{**}P < 0.01$.

NF-κB activation and upregulation of CIDEA and CIDEC in the livers of HFD-fed *Ddah1*^{HKO} mice and PA-treated DDAH1-depleted cells, suggesting that the protective effect of DDAH1 on hepatic steatosis and inflammation was partially dependent on repression of S100A11.

Although our data suggested a novel role for DDAH1 in the regulation of S100A11, the mechanism by which DDAH1 regulates S100A11 in fatty livers remains unclear. Since S100A11 is known as an inducer of inflammatory processes[35], it might be regulated by NF-κB, which is the key regulator of early hepatic

inflammatory recruitment in NAFLD[36,37]. Here, we demonstrated that there is a putative NF-κB binding site in the promoter of S100A11 and transfection with p65 could increase the luciferase activity of S100A11 reporter constructs. The activation of NF-κB by DDAH1 deficiency has been observed in MEF cells[38]. We also found that hepatic *Ddah1* deficiency increased, whereas DDAH1 overexpression decreased, p-p65 and p-IκBα levels in fatty livers. *Ddah1* deficiency also exacerbated NF-κB activation and S100A11 up-regulation in PA-treated primary hepatocytes. Moreover, inhibition of NF-κB by QNZ decreased S100A11 expression in PA-treated *Ddah1*$^{-/-}$ primary hepatocytes. Therefore, these results indicate that DDAH1 may regulate S100A11 through NF-κB-dependent pathway.

JNK also plays an important role in the pathogenesis of NAFLD by promoting insulin resistance and inflammation[39,40]. Inhibition of JNK by SP600125 attenuated IR and liver steatosis in HFD-fed rats[41]. In the present study, liver *Ddah1* deficiency significantly exacerbated JNK phosphorylation in fatty livers and PA-treated primary hepatocytes, while overexpression of DDAH1 repressed JNK signaling. Interestingly, SP600125 decreased S100A11 expression in PA-treated *Ddah1*$^{-/-}$ hepatocytes. Thus, JNK may also be involved in the regulation of S100A11 by DDAH1 in fatty livers.

It is well known that ROS overproduction in fatty livers is strongly associated with dysregulation of lipid metabolism, IR, and activation of NF-κB and JNK[42]. Our recent studies suggested that DDAH1 may function as an antioxidant enzyme in MEF cells[38], $PM_{2.5}$-exposed lungs[43] and aged and diabetic kidneys[44]. Consistent with these reports, we demonstrated that deletion of hepatocyte-specific *Ddah1* increased, while overexpression of DDAH1 decreased superoxide and 4-HNE levels in fatty livers, indicating that DDAH1 also attenuates liver steatosis by inhibiting oxidative stress. Consistent with the previous report that H_2O_2 induces upregulation of S100A11 and nuclear translocation in fibroblasts[45], the increase in the expression of S100A11 in PA-treated *Ddah1*$^{-/-}$ hepatocytes was attenuated by NAC. Furthermore, we found that ADMA increased S100A11 expression in HepG2 cells, while inhibition of DDAH1 activity by mutation of the active site residues decreased the repression effect on S100A11 expression in PA-treated HepG2 cells. Therefore, it is likely that DDAH1 also regulates S100A11 by attenuating oxidative stress and degrading ADMA.

The present study showed that S100A11 overexpression dramatically decreased DDAH1 expression in HepG2 cells, while S100A11 knockdown of S100A11 increased DDAH1 expression in fatty livers and PA-treated HepG2 cells, suggesting that there is mutual regulation between S100A11 and DDAH1. Therefore, the up-regulation of S100A11 and the down-regulation of DDAH1 may form a positive feedback fashion and contribute to the development of NAFLD.

5. Conclusions

Our results provided genetic evidence to support the conclusion that hepatic DDAH1/S100A11 plays an important protective role in the development of NAFLD. Increasing DDAH1 or decreasing S100A11 expression in hepatocytes may serve as new therapeutic strategies for the treatment of NAFLD.

Acknowledgments

This study was supported by grants from National Natural Science Foundation of China (82070250, 32200631), Beijing Natural Science Foundation (5222029, China), China Postdoctoral Science Foundation (2022T150640) and the Fundamental Research Funds for the Central Universities.

Author contributions

Xiyue Shen, Kai Luo and Juntao Yuan conceived the study, designed experiments, acquired and analyzed the data. Junling Gao, Bingqing Cui, and Zhuoran Yu contributed to data collection, data analysis and interpretation. Zhongbing Lu conceived the study, designed experiments, analyzed the data and wrote the manuscript. All the authors read and approved the final manuscript.

Conflicts of interest

The authors declare no conflicts of interest.

Appendix A. Supporting information

Supporting data to this article can be found online at https://doi.org/10.1016/j.apsb.2023.05.020.

References

1. Seen TK, Sayed M, Bilal M, Reyes JV, Bhandari P, Lourdusamy V, et al. Clinical indicators for progression of nonalcoholic steatohepatitis to cirrhosis. *World J Gastroenterol* 2021;**27**:3238–48.
2. Rinella ME. Nonalcoholic fatty liver disease: a systematic review. *JAMA* 2015;**313**:2263–73.
3. Buzzetti E, Pinzani M, Tsochatzis EA. The multiple-hit pathogenesis of non-alcoholic fatty liver disease (NAFLD). *Metabolism* 2016;**65**:1038–48.
4. Younossi ZM, Koenig AB, Abdelatif D, Fazel Y, Henry L, Wymer M. Global epidemiology of nonalcoholic fatty liver disease-meta-analytic assessment of prevalence, incidence, and outcomes. *Hepatology* 2016;**64**:73–84.
5. Ji L, Li Q, He Y, Zhang X, Zhou Z, Gao Y, et al. Therapeutic potential of traditional Chinese medicine for the treatment of NAFLD: a promising drug potentilla discolor bunge. *Acta Pharm Sin B* 2022;**12**:3529–47.
6. Dogru T, Genc H, Tapan S, Aslan F, Ercin CN, Ors F, et al. Plasma fetuin-A is associated with endothelial dysfunction and subclinical atherosclerosis in subjects with nonalcoholic fatty liver disease. *Clin Endocrinol* 2013;**78**:712–7.
7. Dogru T, Genc H, Tapan S, Ercin CN, Ors F, Aslan F, et al. Elevated asymmetric dimethylarginine in plasma: an early marker for endothelial dysfunction in non-alcoholic fatty liver disease?. *Diabetes Res Clin Pract* 2012;**96**:47–52.
8. Boga S, Alkim H, Koksal AR, Bayram M, Ozguven MB, Ergun M, et al. Increased plasma levels of asymmetric dimethylarginine in nonalcoholic fatty liver disease: relation with insulin resistance, inflammation, and liver histology. *J Investig Med* 2015;**63**:871–7.
9. Ferrigno A, Di Pasqua LG, Berardo C, Richelmi P, Vairetti M. Liver plays a central role in asymmetric dimethylarginine-mediated organ injury. *World J Gastroenterol* 2015;**21**:5131–7.
10. Hu T, Chouinard M, Cox AL, Sipes P, Marcelo M, Ficorilli J, et al. Farnesoid X receptor agonist reduces serum asymmetric dimethylarginine levels through hepatic dimethylarginine dimethylaminohydrolase-1 gene regulation. *J Biol Chem* 2006;**281**:39831–8.
11. Mookerjee RP, Mehta G, Balasubramaniyan V, Mohamed Fel Z, Davies N, Sharma V, et al. Hepatic dimethylarginine-dimethylaminohydrolase 1 is reduced in cirrhosis and is a target for therapy in portal hypertension. *J Hepatol* 2015;**62**:325–31.

12. Shah RA, Alkhouri N, Kowdley KV. Emerging drugs for the treatment of non-alcoholic steatohepatitis: a focused review of farnesoid X receptor agonists. *Expert Opin Emerg Drugs* 2020;**25**:251−60.
13. Li T, Feng R, Zhao C, Wang Y, Wang J, Liu S, et al. Dimethylarginine dimethylaminohydrolase 1 protects against high-fat diet-induced hepatic steatosis and insulin resistance in mice. *Antioxid Redox Signal* 2017;**26**:598−609.
14. Hu X, Xu X, Zhu G, Atzler D, Kimoto M, Chen J, et al. Vascular endothelial-specific dimethylarginine dimethylaminohydrolase-1-deficient mice reveal that vascular endothelium plays an important role in removing asymmetric dimethylarginine. *Circulation* 2009;**120**:2222−9.
15. Shen X, Ishaq SM, Wang Q, Yuan J, Gao J, Lu Z. DDAH1 protects against acetaminophen-induced liver hepatoxicity in mice. *Antioxidants* 2022;**11**:880.
16. Wang H, Shen X, Liu J, Wu C, Gao J, Zhang Z, et al. The effect of exposure time and concentration of airborne $PM_{2.5}$ on lung injury in mice: a transcriptome analysis. *Redox Biol* 2019;**26**:101264.
17. Charni-Natan M, Goldstein I. Protocol for primary mouse hepatocyte isolation. *STAR Protoc* 2020;**1**:100086.
18. Yuan J, Yu Z, Gao J, Luo K, Shen X, Cui B, et al. Inhibition of GCN2 alleviates hepatic steatosis and oxidative stress in obese mice: involvement of NRF2 regulation. *Redox Biol* 2022;**49**:102224.
19. Liu S, Yuan J, Yue W, Bi Y, Shen X, Gao J, et al. GCN2 deficiency protects against high fat diet induced hepatic steatosis and insulin resistance in mice. *Biochim Biophys Acta Mol Basis Dis* 2018;**1864**:3257−67.
20. Sobolewski C, Abegg D, Berthou F, Dolicka D, Calo N, Sempoux C, et al. S100A11/ANXA2 belongs to a tumour suppressor/oncogene network deregulated early with steatosis and involved in inflammation and hepatocellular carcinoma development. *Gut* 2020;**69**:1841−54.
21. Hong L, Fast W. Inhibition of human dimethylarginine dimethy laminohydrolase-1 by *S*-nitroso-L-homocysteine and hydrogen peroxide. Analysis, quantification, and implications for hyperhomocysteinemia. *J Biol Chem* 2007;**282**:34684−92.
22. Xu X, Zhang P, Kwak D, Fassett J, Yue W, Atzler D, et al. Cardiomyocyte dimethylarginine dimethylaminohydrolase-1 (DDAH1) plays an important role in attenuating ventricular hypertrophy and dysfunction. *Basic Res Cardiol* 2017;**112**:55.
23. Tomlinson JA, Caplin B, Boruc O, Bruce-Cobbold C, Cutillas P, Dormann D, et al. Reduced renal methylarginine metabolism protects against progressive kidney damage. *J Am Soc Nephrol* 2015;**26**:3045−59.
24. Druhan LJ, Forbes SP, Pope AJ, Chen CA, Zweier JL, Cardounel AJ. Regulation of eNOS-derived superoxide by endogenous methylarginines. *Biochemistry* 2008;**47**:7256−63.
25. Veresh Z, Debreczeni B, Hamar J, Kaminski PM, Wolin MS, Koller A. Asymmetric dimethylarginine reduces nitric oxide donor-mediated dilation of arterioles by activating the vascular renin-angiotensin system and reactive oxygen species. *J Vasc Res* 2012;**49**:363−72.
26. Geisler CE, Renquist BJ. Hepatic lipid accumulation: cause and consequence of dysregulated glucoregulatory hormones. *J Endocrinol* 2017;**234**:R1−21.
27. Du D, Liu C, Qin M, Zhang X, Xi T, Yuan S, et al. Metabolic dysregulation and emerging therapeutical targets for hepatocellular carcinoma. *Acta Pharm Sin B* 2022;**12**:558−80.
28. Herzig S, Hedrick S, Morantte I, Koo SH, Galimi F, Montminy M. CREB controls hepatic lipid metabolism through nuclear hormone receptor PPAR-gamma. *Nature* 2003;**426**:190−3.
29. Xiao X, Song BL. SREBP: a novel therapeutic target. *Acta Biochim Biophys Sin* 2013;**45**:2−10.
30. Kim YH, Barclay JL, He J, Luo X, O'Neill HM, Keshvari S, et al. Identification of carboxypeptidase X (CPX)-1 as a positive regulator of adipogenesis. *FASEB J* 2016;**30**:2528−40.
31. Luo H, Jiang M, Lian G, Liu Q, Shi M, Li TY, et al. AIDA selectively mediates downregulation of fat synthesis enzymes by ERAD to retard intestinal fat absorption and prevent obesity. *Cell Metab* 2018;**27**:843−53.
32. Zhang L, Zhang Z, Li C, Zhu T, Gao J, Zhou H, et al. S100A11 promotes liver steatosis *via* FOXO1-mediated autophagy and lipogenesis. *Cell Mol Gastroenterol Hepatol* 2021;**11**:697−724.
33. Teng F, Jiang J, Zhang J, Yuan Y, Li K, Zhout B, et al. The S100 calcium-binding protein A11 promotes hepatic steatosis through RAGE-mediated AKT−mTOR signaling. *Metabolism* 2021;**117**:154725.
34. Calderaro J, Couchy G, Imbeaud S, Amaddeo G, Letouzé E, Blanc JF, et al. Histological subtypes of hepatocellular carcinoma are related to gene mutations and molecular tumour classification. *J Hepatol* 2017;**67**:727−38.
35. He H, Li J, Weng S, Li M, Yu Y. S100A11: diverse function and pathology corresponding to different target proteins. *Cell Biochem Biophys* 2009;**55**:117−26.
36. Cai D, Yuan M, Frantz DF, Melendez PA, Hansen L, Lee J, et al. Local and systemic insulin resistance resulting from hepatic activation of IKK-β and NF-κB. *Nat Med* 2005;**11**:183−90.
37. Guo Y, Zhang X, Zhao Z, Lu H, Ke B, Ye X, et al. NF-κB/HDAC1/SREBP1c pathway mediates the inflammation signal in progression of hepatic steatosis. *Acta Pharm Sin B* 2020;**10**:825−36.
38. Zhao C, Li T, Han B, Yue W, Shi L, Wang H, et al. DDAH1 deficiency promotes intracellular oxidative stress and cell apoptosis *via* a miR-21-dependent pathway in mouse embryonic fibroblasts. *Free Radic Biol Med* 2016;**92**:50−60.
39. Vernia S, Cavanagh-Kyros J, Garcia-Haro L, Sabio G, Barrett T, Jung DY, et al. The PPARα−FGF21 hormone axis contributes to metabolic regulation by the hepatic JNK signaling pathway. *Cell Metab* 2014;**20**:512−25.
40. Tarantino G, Caputi A. JNKs, insulin resistance and inflammation: a possible link between NAFLD and coronary artery disease. *World J Gastroenterol* 2011;**17**:3785−94.
41. Yan H, Gao Y, Zhang Y. Inhibition of JNK suppresses autophagy and attenuates insulin resistance in a rat model of nonalcoholic fatty liver disease. *Mol Med Rep* 2017;**15**:180−6.
42. Pedroza-Diaz J, Arroyave-Ospina JC, Serna Salas S, Moshage H. Modulation of oxidative stress-induced senescence during non-alcoholic fatty liver disease. *Antioxidants* 2022;**11**:975.
43. Gao J, Lei T, Wang H, Luo K, Wang Y, Cuit B, et al. Dimethylarginine dimethylaminohydrolase 1 protects $PM_{2.5}$ exposure-induced lung injury in mice by repressing inflammation and oxidative stress. *Part Fibre Toxicol* 2022;**19**:64.
44. Shi L, Zhao C, Wang H, Lei T, Liu S, Caot J, et al. Dimethylarginine dimethylaminohydrolase 1 deficiency induces the epithelial to mesenchymal transition in renal proximal tubular epithelial cells and exacerbates kidney damage in aged and diabetic mice. *Antioxid Redox Signal* 2017;**27**:1347−60.
45. Kozlov SV, Waardenberg AJ, Engholm-Keller K, Arthur JW, Graham ME, Lavin M. Reactive oxygen species (ROS)-activated ATM-dependent phosphorylation of cytoplasmic substrates identified by large-scale phosphoproteomics screen. *Mol Cell Proteom* 2016;**15**:1032−47.